NOTES AND CORRESPONDENCE

Empirical Orthogonal Functions and Multiple Flow Regimes in the Southern Hemisphere Winter

JOHN D. FARRARA, MICHAEL GHIL* AND CARLOS R. MECHOSO

Climate Dynamics Center and Department of Atmospheric Sciences, University of California, Los Angeles, California

KINGTSE C. MO

Climate Analysis Center, National Meteorological Center, NWS/NOAA, Washington, DC

15 November 1988 and 2 June 1989

ABSTRACT

We present a new empirical orthogonal function (EOF) analysis of winter 500 mb geopotential height anomalies in the Southern Hemisphere. An earlier EOF analysis by two of the present authors prefiltered the anomalies to exclude wavenumbers 5 and higher; we do not. The different preprocessing of data affects the results. All three distinct planetary flow regimes identified in the winter circulation of the Southern Hemisphere by a pattern correlation method are captured by the new set of EOFs; only two of those regimes were captured by the earlier set. The new results, therefore, lend further support to the idea that EOFs point to distinct planetary flow regimes.

1. Introduction

Recurrent, quasi-stationary circulation patterns that persist beyond the periods typical of synoptic-scale variability have been the subject of many recent observational studies. Dole and Gordon (1983) and Horel (1985), using different methods, identified such persistent patterns in daily 500 mb geopotential height fields during Northern Hemisphere (NH) winter, and classified them into several hemispheric flow regimes. Mo (1986), using the objective persistence criterion of Horel (1985), identified persistent events in the 1972–83 dataset of winter 500 mb geopotential heights for the Southern Hemisphere (SH) produced by the World Meteorological Centre in Melbourne, Australia. The flow patterns during these SH events fell into one of three distinct flow regimes. The first two of these flow regimes show a large zonal wavenumber 3 component and differ in the relative importance of the zonal wavenumber 1 component. The third flow regime shows a large zonal wavenumber 4 component.

Mo and Ghil (1987; hereafter MG) investigated the relation between the empirical orthogonal functions (EOFs) of the Australian set of 500 mb geopotential heights and the multiple flow regimes in the SH. The first two EOFs in MG were associated with flow regimes identified by Mo (1986). The third EOF in MG was called the Pacific–South American (PSA) pattern because it is nearly a mirror image about the equator of the Pacific–North American (PNA) pattern (Horel and Wallace 1981). EOFs beyond the third are not discussed in MG. Therefore, one of the persistent flow regimes in Mo (1986) is not associated with any of the EOFs in MG.

In the course of a study on standing and traveling planetary-scale disturbances in the SH stratosphere and troposphere during winter (Mechoso, Farrara, and Ghil; personal communication 1988), we have carried out an EOF analysis of 500 mb geopotential height anomalies using a different dataset and analysis procedure. In the new set of EOFs, all of the persistent flow regimes identified by Mo (1986), as well as the PSA pattern, are represented. These new results lend further support to the relationship established in MG between statistics and nonlinear dynamics of the SH winter circulation. This relationship was also illustrated for the NH winter circulation by Mo and Ghil (1988).

2. Data and methods

The dataset used here consists of the U.S. National Meteorological Center (NMC) daily 1200 UTC analyses of geopotential height at 500 mb covering the 92-day SH winter seasons (June–August) of 1979–85. This dataset overlaps with the one used by MG for the winters of 1979–83. To perform the EOF analysis the fields

* Also affiliated with the Institute of Geophysics and Planetary Physics, UCLA.

Corresponding author address: Dr. John D. Farrara, Department of Atmospheric Sciences, University of California, 405 Hilgard Avenue, Los Angeles, CA 90024.

are first transformed from the original 5° × 2.5° longitude–latitude grid to the 380 point grid of Barnston and Livezey (1987), which has approximately equal distances between points. The seven-winter grand mean defined with respect to time is then subtracted from the daily fields yielding a set of daily anomalies at each grid point. The EOFs are the eigenvectors of the 380 × 380 covariance matrix thus obtained. The covariances are computed based on the daily anomalies, as defined in this paragraph—no low-pass filtering in time is applied.

There are three differences between the procedures followed in MG and here:

1) Mo and Ghil removed the annual and semiannual components of the seasonal cycle from the raw geopotential heights to produce the anomaly fields, while we remove the seven-winter averages.

2) Mo and Ghil divided the raw geopotential height anomalies at each grid point by their standard deviation for the winter season, while we analyze the raw geopotential height anomaly fields; i.e., we analyze the covariance, rather than the correlation matrix.

3) Mo and Ghil applied the EOF analysis to the geopotential height anomalies *restricted to zonal wavenumbers zero through 4* at each latitude (compare also Horel 1985).

As we shall see in section 3, an interesting difference arises between the two analyses. In order to narrow down the reasons for this difference, we also carried out an eigenanalysis of the correlation matrix for our dataset; i.e., we also considered the standardized anomalies. The order of the EOFs is the same in both cases, and the patterns are substantially the same, with a slight drift of the extrema in each pattern towards lower latitudes in the case of the standardized anomalies.

3. Results

The first, second, and fourth EOFs obtained with our procedure have counterparts among the EOFs in MG (see Table 1 and Fig. 1). Our first EOF (Fig. 1a), which contains 12.6 ± 1.5% of the total variance of the field, is similar to the composite of three quasi-stationary events with large amplitude of zonal wavenumber 3 and significant amplitude of zonal wavenumber 1, shown in Fig. 10b of Mo (1986) and in Fig. 11b of MG. Its phase reversal with latitude, also observed by Rogers and van Loon (1982), is most likely related to the interannual variability of the seasonal cycle (van Loon 1967). Our second EOF (Fig. 1b), which contains 9.1 ± 1.0% of the total variance of the field, is similar to the PSA pattern in MG. Our fourth EOF (Fig. 1d), which contains 7.4 ± 0.7% of the total variance of the field, is similar to the composite of persistent events shown in Fig. 9b of Mo (1986) and in Fig. 11a of MG, with large amplitude of zonal wavenumber 3, its zonal phase in high latitudes nearly opposite to that of our first EOF (Fig. 1a), and a much smaller wavenumber 1 component.

On the other hand, our third EOF (Figs. 1c and 2a), which accounts for 8.1 ± 0.9% of the total variance of the field, does not resemble any of the previously published EOFs for the SH. This EOF is almost identical to the composite of four quasi-stationary events of 500 mb height anomalies dominated by a zonal wavenumber 4 pattern, presented by Mo (1986, Fig. 8b) and reproduced in Fig. 2b here. The overlapping error bars of our second, third and fourth EOFs suggest degeneracy between them. As explained in MG, this is not a problem if the underlying dynamics can be seen to have distinct modes of variability with comparable variances. The association of these EOFs with the distinct flow regimes identified by Mo (1986) is sufficient to remove the suspicion of degeneracy.

In order to narrow down the reasons for the indicated discrepancy with MG, we have also determined EOFs of the anomalies in our dataset filtered to retain only zonal wavenumbers zero through 4. The first three EOFs in this case correspond to those in MG (see Table 1). Furthermore, none of the higher-order EOFs in this set have the structure of the third EOF we obtained from the unfiltered anomalies. Thus, the absence of this pattern from the set of EOFs in MG is apparently due to the neglect of the flow components with zonal wavenumbers larger than 4, i.e., to a truncation and aliasing effect.

There are two interesting questions which arise at this point:

(i) Why does an EOF analysis based on zonal wavenumbers zero through 4 fail to capture an EOF dominated by wavenumber 4?

(ii) How is it that the proportion of variance accounted for by three EOFs (1, 4 and 2) of the unfiltered dataset, 29% of the total, exceeds the variance associated with the corresponding three EOFs (1, 2, and 3) of the filtered dataset, 21% of the total?

A complete answer is beyond the scope of the present note. But we can at least indicate why these two facts are less counterintuitive than they appear at first sight.

Concerning the first question, the power spectrum of the principal component (PC) associated with our third EOF, i.e., of the time series of its coefficients, is shown in Fig. 3. It is clear that most of the power lies below the synoptic time scale of two to ten days. In particular, interesting peaks appear at 15 and 26 days. Thus EOF 3 is indeed associated with low-frequency variability (LFV) of the SH winter atmosphere, reinforcing the result that its spatial pattern resembles that of one set of recurrent, persistent anomalies characterizing this LFV.

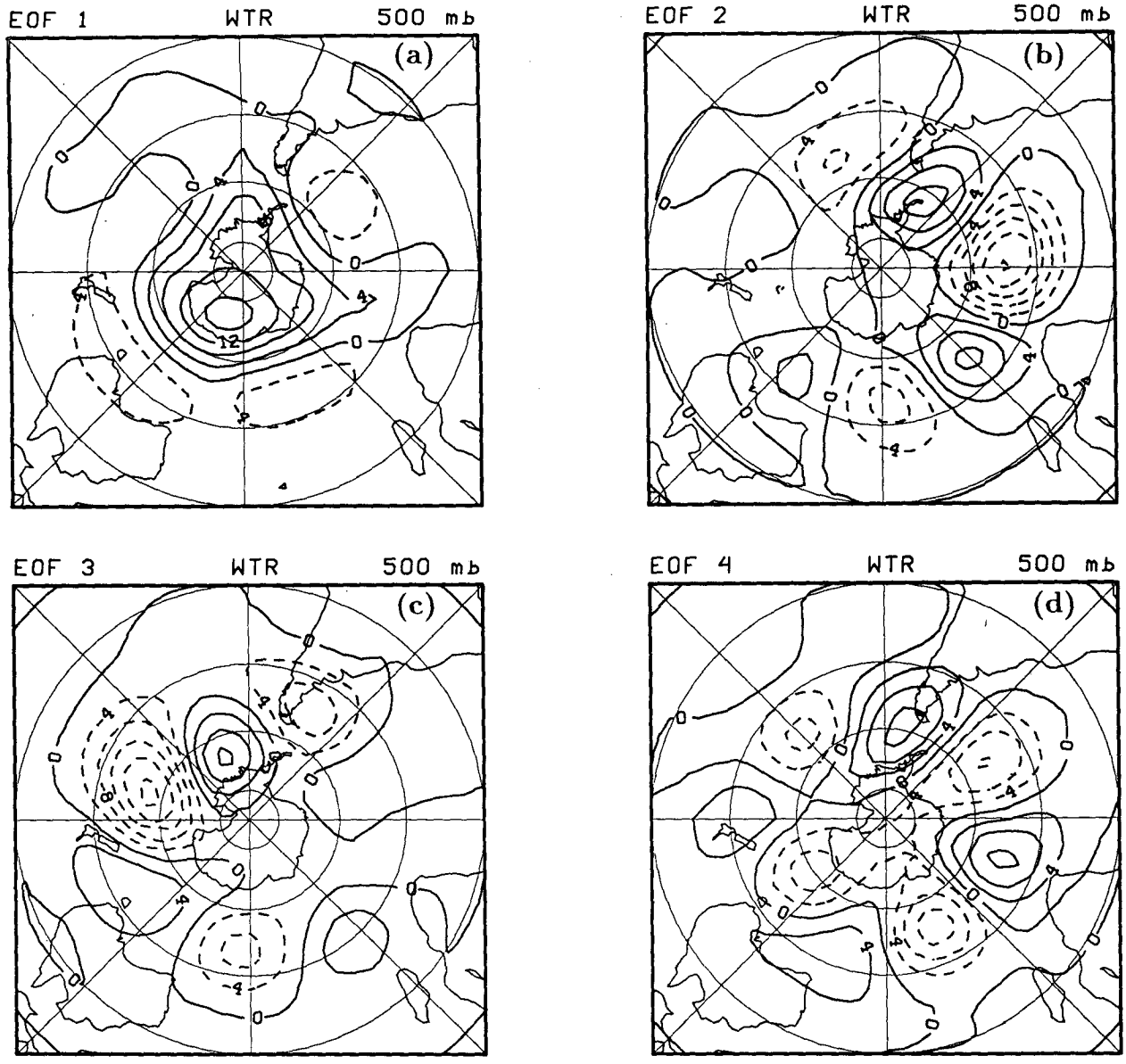

FIG. 1. The leading four EOFs, panels (a)–(d), of the time series of 500 mb geopotential height anomalies during seven SH winters. EOFs normalized to unit vector length × 100; contour interval is four nondimensional units.

It turns out that the higher-order EOFs (not shown) are dominated by wavenumbers 4, 5 and 6, with weaker components of zero through 3. This helps explain why the two leading EOFs dominated by zonal wavenumbers 1 and 3, as well as that associated with the strongly localized PSA pattern, were not affected by the filtering, while EOF 3 of the unfiltered dataset, being dominated by zonal wavenumber 4, was aliased out of the filtered dataset.

This aliasing can be explained as follows. The time series of anomaly maps $\phi(\lambda, \theta, t)$, where λ is longitude, θ is latitude, and t is time, can be expanded either into a Fourier series at each latitude or into an EOF series. If both series are infinite, in particular if the EOFs have been determined from the full anomalies, then the complete separation of variables, i.e., the expansion into a double series

$$\phi(\lambda, \theta, t) = \sum_{j=1}^{\infty} \sum_{k=-\infty}^{\infty} a_{jk}(t) b_{jk}(\theta) e^{ik\lambda} \qquad (1)$$

obtained from either expansion will be the same, by the orthogonality of the EOFs and of the complex exponentials, respectively. However, prior truncation or

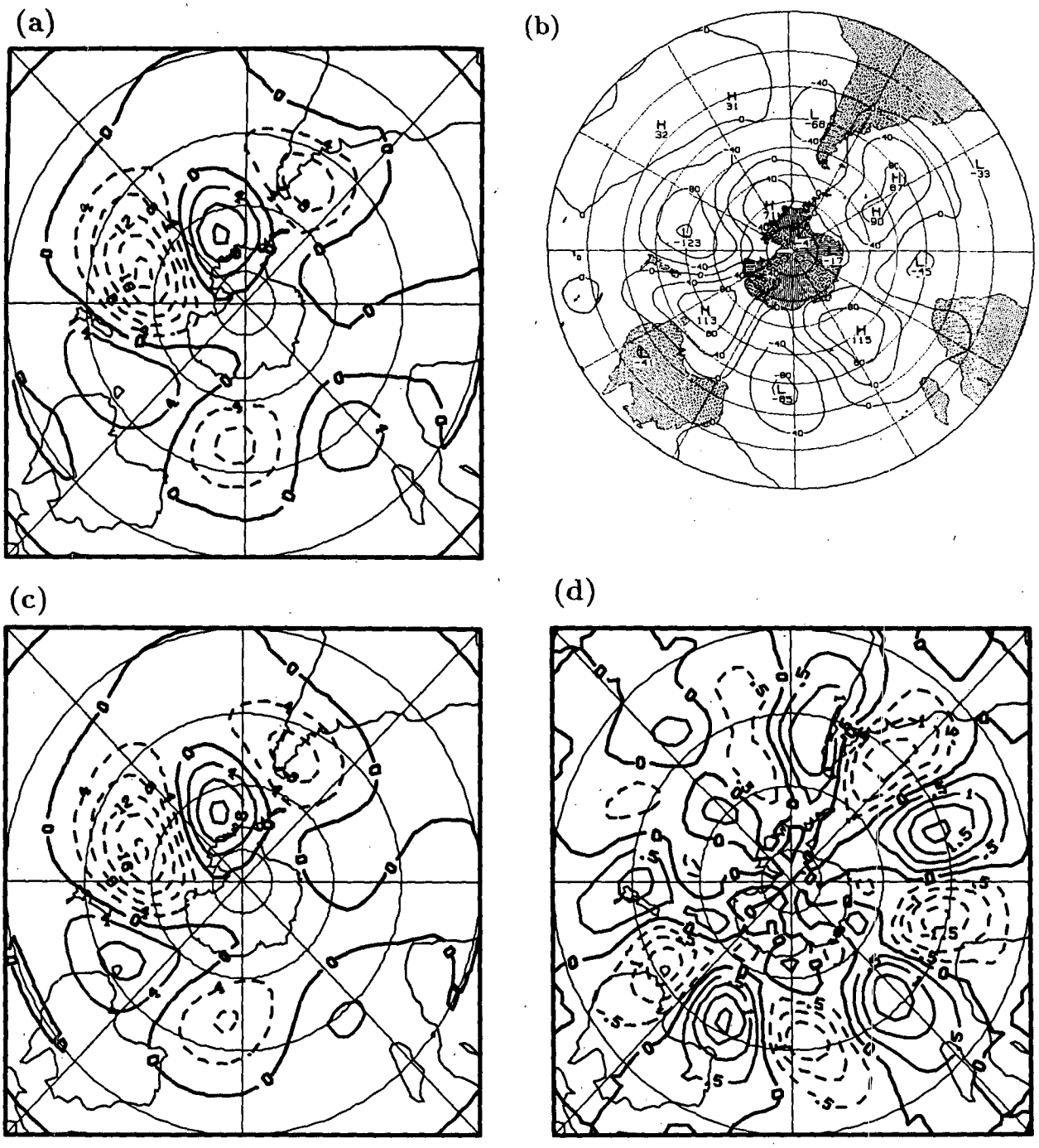

FIG. 2. (a) EOF 3 (same as Fig. 1c); (b) total anomalies of a composite map of four quasi-stationary events with a large zonal wavenumber 4 amplitude (from Mo 1986); (c) projection of EOF 3 onto the first four zonal wavenumbers; (d) difference between panels (a) and (c). Contour interval for panels (a) and (c) is four nondimensional units; for panel (d) it is 0.5 units.

filtering of the anomaly fields in wavenumber will lead to a different covariance matrix. The operations summarized in Eq. (1) are all linear, and the two summations can be interchanged if the double series converges (which we expect to be the case in practice). However, the computation of the covariances is quadratic in the Fourier coefficients, and the solution of the eigenproblem is highly nonlinear in the elements of the covariance matrix. Hence the aliasing.

These ideas are supported by the information pre-

sented in Figs. 2c, d. The projection of the third EOF of the unfiltered dataset onto zonal wavenumbers zero through 4 [panel (c)] differs only very slightly from the EOF itself (Fig. 2a). But the difference, shown in panel (d), while small, exhibits a systematic pattern dominated by zonal wavenumbers 5 and 6. This indicates that the intermediate wavenumbers 4, 5 and 6 are inextricably linked together in the SH winter circulation, and that this variability is severely distorted by retaining only zonal wavenumbers zero through 4.

Concerning the second question, all that can be said with certainty is that the *total* variance of the filtered dataset has to be less than that of the unfiltered one. *If* the partial variance in each leading EOF were the same absolute number, then its *relative* contribution to the total filtered variance would have to be larger than its fraction of the unfiltered one. This is not the case for our dataset. We suspect that this is so because of the relative importance of intermediate wavenumbers 4 through 7 in the SH atmosphere. The subtraction of much of their variance from the filtered dataset distorts substantially the entire picture, leaving us at a loss as to the complete answer to the second question.

4. Summary

Mo and Ghil (1987) associated two persistent flow regimes, dominated by distinct zonal wavenumber 3 patterns (Mo 1986), with two leading EOFs of the SH 500 mb winter geopotential height field. In this note, we showed that if zonal wavenumbers greater than 4 are retained, all three of Mo's persistent regimes can be associated with leading EOFs. These results reinforce the idea, proposed by Ghil (1987, 1988), that EOFs tend to point to distinct planetary flow regimes which include the most persistent, quasi-stationary circulation patterns.

TABLE 1. EOFs and multiple flow regimes in the SH.

Flow regime	EOF		
		Present analysis	
	MG	Unfiltered	Filtered
Waves 3, 1	1, 10.8 ± 1.2%	1, 12.6 ± 1.5%	1, 9.4 ± 0.9%
Wave 3	2, 6.8 ± 0.7%	4, 7.4 ± 0.7%	2, 5.8 ± 0.5%
PSA	3, 5.4 ± 0.4%	2, 9.1 ± 1.0%	3, 5.4 ± 0.5%
Wave 4	not present	3, 8.1 ± 0.9%	not present
Total	23%	29.1% (37.2%)*	20.6%

* Without 3 (with 3 in parentheses).

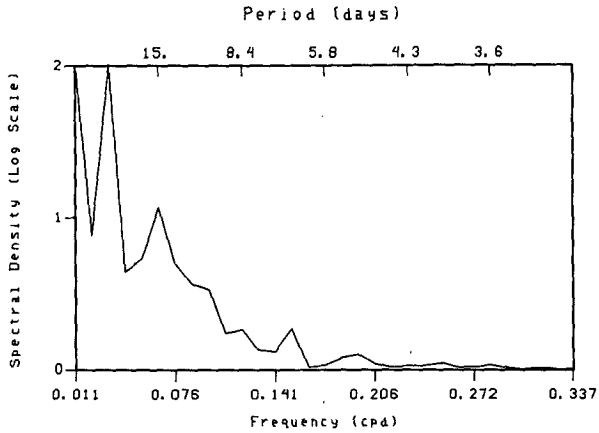

FIG. 3. Power spectrum of PC 3.

Acknowledgments. It is a pleasure to thank John D. Horel and one anonymous reviewer for helpful comments and constructive suggestions. Support for this work was provided by NASA under Grants NAGW-1021 and NAG-5713, and by NSF under Grant ATM-861542.

REFERENCES

Barnston, A. G., and R. E. Livezey, 1987: Classification, seasonality and persistence of low-frequency atmospheric circulation patterns. *Mon. Wea. Rev.*, **115**, 1083–1126.

Dole, R. M., and N. D. Gordon, 1983: Persistent anomalies of the extratropical Northern Hemisphere wintertime circulation: Geographical distribution and regional characteristics. *Mon. Wea. Rev.*, **111**, 1567–1586.

Ghil, M., 1987: Dynamics, statistics and predictability of planetary flow regimes. *Irreversible Phenomena and Dynamical Systems Analysis in Geosciences.* C. Nicolis and G. Nicolis, Eds., D. Reidel, 241–283.

——, 1988: Nonlinear approaches to low-frequency atmospheric variability. *Dynamics of Low-Frequency Phenomena in the Atmosphere.* G. W. Branstator, R. A. Madden and J. J. Tribbia, Eds., National Center for Atmospheric Research, 603–714.

Horel, J. D., 1985: Persistence of the 500 mb height field during Northern Hemisphere winter. *Mon. Wea. Rev.*, **113**, 2030–2042.

——, and J. M. Wallace, 1981: Planetary-scale atmospheric phenomena associated with the Southern Oscillation. *Mon. Wea. Rev.*, **109**, 813–829.

Mo, K. C., 1986: Quasi-stationary states in the Southern Hemisphere. *Mon. Wea. Rev.*, **114**, 808–823.

——, and M. Ghil, 1987: Statistics and dynamics of persistent anomalies. *J. Atmos. Sci.*, **44**, 877–901.

——, and ——, 1988: Cluster analysis of multiple planetary flow regimes. *J. Geophys. Res.*, **93D**, 10 927–10 952.

Rogers, J. C., and H. van Loon, 1982: Spatial variability of sea-level pressure and 500 mb height anomalies over the Southern Hemisphere. *Mon. Wea. Rev.*, **110**, 1375–1392.

van Loon, H., 1967: The half yearly oscillations in middle and high southern latitudes and the coreless winter. *J. Atmos. Sci.*, **24**, 472–486.